



**University of
Zurich**^{UZH}

**Zurich Open Repository and
Archive**

University of Zurich
University Library
Strickhofstrasse 39
CH-8057 Zurich
www.zora.uzh.ch

Year: 2013

Two-photon microscopy with double-circle trajectories for in vivo cerebral blood flow measurements

Landolt, Andrin ; Obrist, Dominik ; Wyss, Matthias ; Barrett, Matthew ; Langer, Dominik ; Jolivet, Renaud ; Soltysinski, Tomasz ; Roesgen, Thomas ; Weber, Bruno

DOI: <https://doi.org/10.1007/s00348-013-1523-5>

Posted at the Zurich Open Repository and Archive, University of Zurich

ZORA URL: <https://doi.org/10.5167/uzh-93362>

Journal Article

Originally published at:

Landolt, Andrin; Obrist, Dominik; Wyss, Matthias; Barrett, Matthew; Langer, Dominik; Jolivet, Renaud; Soltysinski, Tomasz; Roesgen, Thomas; Weber, Bruno (2013). Two-photon microscopy with double-circle trajectories for in vivo cerebral blood flow measurements. *Experiments in Fluids*, 54(5):1523-1530.

DOI: <https://doi.org/10.1007/s00348-013-1523-5>

Two-photon microscopy with double-circle trajectories for in vivo cerebral blood flow measurements

Andrin Landolt · Dominik Obrist · Matthias Wyss · Matthew Barrett ·
Dominik Langer · Renaud Jolivet · Tomasz Soltysinski · Thomas
Roesgen · Bruno Weber

Received: 31 October 2012 / Accepted: 15 April 2013

Abstract Scanning microscopes normally use trajectories which produce full-frame images of an object at a low frame rate. Time-resolved measurements are possible if scans along a single line are repeated at a high rate. In conjunction with fluorescence labeling techniques, in vivo recording of blood flow in single capillaries is possible. The present work investigates scanning with double-circle trajectories to measure blood flow simultaneously in several vessels of a capillary network. With the trajectory centered near a bifurcation, a double-circle crosses each vessel twice, creating a sensing gate for passing dark red blood cells in fluorescently labeled plasma. From the stack of scans repeated at 1300 Hz, the time-resolved velocity is retrieved using an image correlation approach. Single bifurcation events can be identified from a few fluorescently labeled red blood cells.

The applicability of the method for in vivo measurements is illustrated on the basis of two-photon laser scanning microscopy of the cerebral capillary network of mice. Its performance is assessed with synthetic data generated from a two-phase model for the perfusion in a capillary network. The calculation of velocities is found to be sufficiently robust for a wide range of conditions. The achievable limits depend significantly on the ex-

perimental conditions and are estimated to be in the 1 $\mu\text{m/s}$ (velocity) and 0.1 s (time resolution) ranges, respectively. Some manual fine-tuning is required for optimal performance in terms of accuracy and time-resolution. Further work may lead to improved reliability with which bifurcation events are identified in the algorithm and to include red blood cell flux and hematocrit measurements.

With the capability for time-resolved measurements in all vessels of a bifurcation, double-circle scanning trajectories allow a detailed study of the dynamics in vascular networks.

Keywords cerebral microcirculation · scanning two-photon microscopy · particle image velocimetry

1 Introduction

Two-photon laser scanning microscopy is a method for three-dimensional fluorescence imaging [1]. In combination with in vivo fluorescence labeling techniques it can provide data from living tissue several hundred microns below the surface and has found wide applications in cellular imaging [2]. In contrast to more traditional optical microscopy techniques (e.g. confocal microscopy), two-photon microscopy relies on the non-linear excitation of a molecule by the simultaneous absorption of two photons. The necessary high spatial photon density is generated by tightly focusing an ultra-short laser pulse. With this, two-photon absorption remains confined to a region close to the focal point [2]. Because the quantum energies of two photons are combined in the absorption process, the emission occurs at a shorter wavelength than the excitation. Common fluorescent markers can therefore be excited in the near-infrared range where light penetrates deeper into tissue. Both features make

A. Landolt · D. Obrist · T. Roesgen
Institute of Fluid Dynamics, ETH Zurich
8092 Zurich, Switzerland
E-mail: landolt@ifd.mavt.ethz.ch

M. Wyss · M. Barrett · R. Jolivet · T. Soltysinski · B. Weber
Institute of Pharmacology and Toxicology, University of Zurich
8057 Zurich, Switzerland

D. Langer
Brain Research Institute, University of Zurich
8057 Zurich, Switzerland

the method less sensitive to scattering and allows for high-resolution imaging at higher penetration depths.

Time-resolved in vivo measurements of blood flow in capillary networks at a spatial resolution of single vessels are of great importance in many fields such as neurobiology and tumor research. It is possible to measure blood flow at the capillary level using single-photon excited fluorescence microscopy. However, its depth-resolution is rather poor and it is inaccurate for vessels that are not perpendicular to the optical axis [3]. The full-field acquisition rate of scanning microscopes in the range of 1 frame per second is too slow for time-resolved measurements. With an axial line-scanning (LS) approach for two-photon microscopy, Kleinfeld et al. [4] achieved time-resolved measurements of red blood cell (RBC) velocity and flux in individual capillaries of a rat neocortex. In LS, data is collected by repeatedly scanning along a single vessel at a high rate. The plasma is stained with a fluorescent large molecular weight compound (e.g. dextran) so that non-fluorescent areas can be associated with traveling red blood cells (RBCs). This permits to determine speed and cell density from the pattern in the stacked lines. Kleinfeld et al. [4] measured RBC velocities with magnitudes between 0 to 1 mm/s from an average of 50 lines or an interval of 0.1 s, respectively. The authors observed effects of sensory stimulations on blood flow in individual capillaries and an essentially incoherent flow distribution in capillary sections that include a bifurcation. These findings suggest that the dynamics of blood flow at the capillary level is actively regulated and relevant for neurobiology. Moreover, the presence of contractile pericytes at bifurcation points (Peppiatt et al. [7]) suggests that branching points in the capillary network could be an important site for active regulation. There is thus an interest in simultaneously measuring flow in all capillaries branching from a node. Kamoun et al. [3] used residence time line scanning (RTLS) with the scanning line at an arbitrary angle to the vessel. The method can measure simultaneously in multiple vessels if they cross the linear scanning trajectory and was reported to be in good agreement with LS data. In the same study, the authors presented relative velocity field scanning (RVFS), a full-field approach that allows the simultaneous measurement of RBC velocity, flux, hematocrit and shear rate in most of the vessels in the field of view. This comes at the cost of temporal resolution as multiple scan angles and speeds are required.

Curved trajectories can further extend the capabilities of laser scanning microscopes. In this work, double circle trajectories for blood flow measurements in a cerebral capillary network are investigated. With the microscope scanning alternately along an inner and an

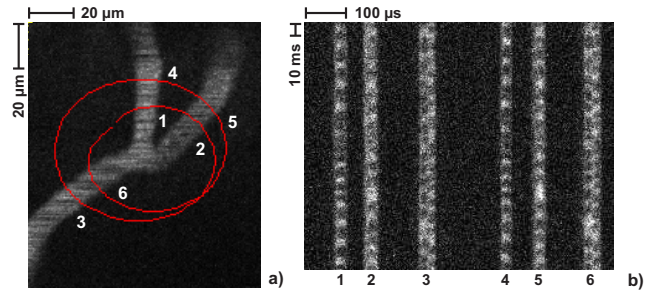


Fig. 1 Anatomical two-photon microscope image of (a) a bifurcation in the cerebral capillary network of mice and (b) a 200 line excerpt of double-circle trajectory data from 150 ms of measurement time. Scanning starts at the upper left corner of the image, with each row of 250 pixels representing one full double circle. Each branch of the bifurcation is represented by two vertical stripe patterns in the double-circle data (the correspondence is illustrated with numbers; note the different time scale along the two image axes).

outer circle centered on a bifurcation, each vessel is crossed twice in a short time interval and at two different locations. This creates a sensing gate for passing RBCs and permits to measure simultaneously the time-resolved RBC velocity magnitude and direction in each vessel. The adaptation of an existing setup for non-linear beam trajectories is relatively straightforward, as only the software has to be modified which drives the piezoelectric mirrors to guide the optical path.

2 Methods

In every scan cycle, a double-circle trajectory that is centered on a bifurcation intersects each vessel twice at two different locations (Figure 1a). Subsequent scanning at a high rate yields a stack of lines as shown in Figure 1b wherein the crossings of all three vessels are discernible as six vertical bands. The bright areas indicate stained plasma while dark areas are associated with the passage of non-fluorescent RBCs. Comparing and matching sequences of dark and bright sections in two corresponding bands allows to determine the distance and time-interval between the two passages and with this the RBC velocity. Additionally tagging a sufficiently small fraction of RBCs (i.e. staining with a fluorescent cell linker) permits to identify and follow the passage of single RBCs through the bifurcation and relate the RBC path to the velocities in the three branches.

For post-processing, the three branches of the bifurcation are treated sequentially by extracting the two corresponding vertical stripes (e.g. 1 and 4 in Figure 1b) from the stack. The two stripe patterns of passing RBCs are then matched piecewise against each other using an image correlation approach. We use a Particle Im-

age Velocimetry (PIV) algorithm with grid refinement [5] to maximize the (time) resolution. An approximate width and horizontal position from both stripes of each capillary is determined based on the vertically averaged intensity distribution in the image. Care is taken that the selections are several pixels wider than the capillary images. The respective sections are then extracted pairwise and vertically divided into sub-windows of suitable length and overlap for image correlation (Figure 2a). In the horizontal direction a single window of fixed width is used while the vertical initial window length of typically 1024 pixel is gradually reduced in three PIV-iterations, where the calculated shifts are used as initial guess for the next pass to minimize the pixel search range. The minimum search window size is currently adapted manually with respect to RBC speed and image quality to give a good compromise between error and time resolution. The vertical window overlap is set to half the window length. The image coordinate pair $((i_0, j_0)$ and (i_1, j_1) in Figure 2), which represents the two intersections of trajectory and vessel, is obtained by adding the calculated PIV sub-pixel shift to the position in the original stack.

Each pixel position in the measurement image can then be associated with a time (Figure 2b) and a position in physical space (Figure 2c and d). The time matrix is constructed using the scanning rate and resolution set for the measurement while the position is retrieved from the recorded mirror position signal (converted to physical space with off-line calibration data from the microscope). The values corresponding to the pixel positions (i_0, j_0) and (i_1, j_1) are calculated by linear neighborhood interpolation in the time and position matrices. From this, the time interval Δt and the distance Δx between two passages of the scanning beam can be accurately determined for each vessel. The instantaneous RBC velocities are finally found from $v = \Delta x / \Delta t$.

Individual bifurcation events are detected from stained RBCs recorded in a separate (green) channel (Figure 2e) by morphological image processing and centroid computation. As the two channels (red and green) are captured simultaneously, it is possible to relate single bifurcation events to the instantaneous flow velocities in the bifurcation. With low contrast in the green channel and significant variation of RBC velocity and image quality between datasets in data collected in vivo, checking by the user is necessary to avoid overlooking bifurcation events or detecting false events. Similar to LS, the data permits to determine linear RBC density and flux [4] but the related processing steps are not yet implemented.

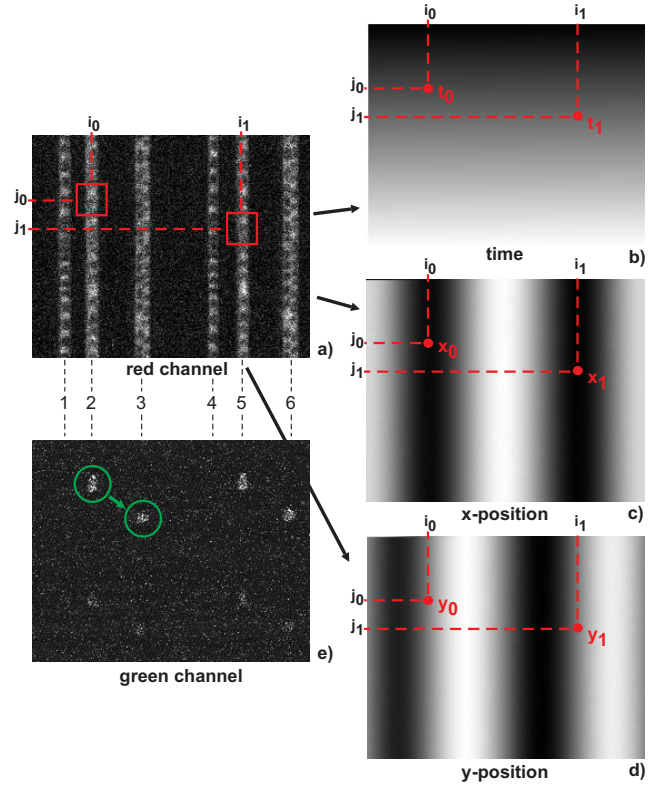


Fig. 2 Post-processing of the double-circle data: (a) Identification and location of a characteristic sequence in the two patterns representing the two crossings of a vessel by the trajectory using a PIV-style image correlation method with sub-pixel accuracy on the red channel. From the pixel coordinates, time (b) and position (c) and (d) of the crossings are determined with a time matrix based on scanning rate and resolution and the recorded x and y mirror position signals. The simultaneously recorded green channel (e) allows identifying single bifurcation events. Here the transition of a RBC from capillary 2 to 3 is highlighted.

For high accuracy, the double-circle trajectory has to intersect the capillaries at close to 90 degrees and with a maximum distance between the two circles while remaining within the acceleration limits of the scanning mirrors. We propose a trajectory of the following form with smooth transition between inner and outer circle:

$$\begin{aligned} x(\theta) &= x_c + R(\theta) \cos(2\theta + \theta_0) \\ y(\theta) &= y_c + R(\theta) \sin(2\theta + \theta_0) \\ R(\theta) &= R_0 + \Delta R [\tanh(w\theta) - \tanh(w(\theta - \pi)) \\ &\quad + \tanh(w(\theta - 2\pi))] \end{aligned} \quad (1)$$

where the angle θ varies between 0 and 2π , $R_0 = 3 \cdot 10^{-5}$ m, $\Delta R = 10^{-5}$ m and $w = 2$. For the synthetic scan data obtained from a simulation, the center coordinates x_c and y_c coincide with the intersection of the capillaries and the orientation angle θ_0 is 60° (Figure 3a). In the in vivo experiment, the values are set manually based on the anatomical image acquired prior to the

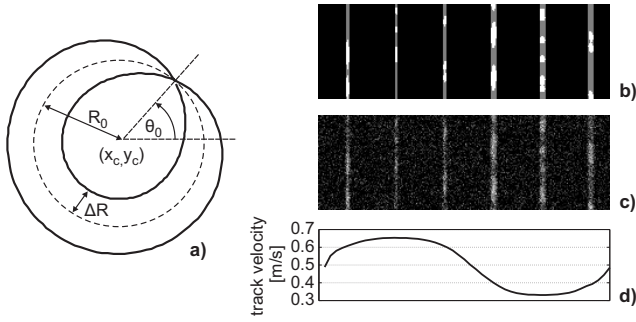


Fig. 3 (a) The proposed double-circle trajectory according to equation (1), (b) synthetic data generated based on numerical simulation of a capillary network and (c) the same data deteriorated with added noise and blur to match the SNR of the experimental data. (d) Shows the variation in track velocities along the trajectory that causes the difference in capillary diameter (visible in panel (b)).

measurement and using the graphical user interface of the software (Figure 1a). Care is thereby taken that the capillaries are orthogonal to the trajectory and that the distance between crossing of inner and outer circle and capillaries is maximized. The maximum velocity that can be measured is estimated by the distance between inner and outer circle divided by half the time interval for one complete trajectory. This estimate yields a maximum measurable velocity of 5 mm/s when scanning at 1300 Hz and with a trajectory according to equation (1).

Both experimental and synthetic datasets were used for development and characterization of the method. The experimental data were obtained from the cerebral cortical capillary network of Isoflurane anesthetized mice with the use of a two-photon scanning microscope. A small craniotomy was performed on the animals above the somatosensory cortex. The cranial window was then covered with agar and a round glass coverslip. To label the plasma fraction, dextran conjugated Texas Red (Sigma-Aldrich; St. Louis MO, USA) was dissolved in saline solution and injected through a venous catheter. Prior to imaging, a small volume of blood was drawn from the animal and RBCs were separated from the plasma fraction by centrifugation and stained with a green fluorescent cell linker (PKH67, Sigma-Aldrich). The stained RBCs were then injected together with the first batch of Texas Red dextran.

Two-photon microscopy was performed using a custom-built microscope with a 16x (0.8 NA, Nikon, Japan) or 20x (1.0 NA, Zeiss GmbH, Germany) water immersion objective. Fluorescence was excited at 870 nm (~ 150 fs pulse duration) with a titanium sapphire laser (Chameleon Ultra II, Coherent Inc., USA). The fluorescent emission was collected simultaneously in two spectral channels with red (590-650 nm) and green (535-550

nm) emission filters. The control of the microscope's motorized stages, mirror scanning and the acquisition of the photomultiplier signal were achieved with LabVIEW software. Anatomical imaging (Figure 1a) was performed at a resolution of 256x256 pixels with averaging over three to five frames. The double circle scans were acquired at a resolution of 250 pixels per cycle with a cycle frequency of 1300 Hz. A total of 40,000 lines were typically recorded for one measurement. With the signal and noise amplitude estimated from the standard deviation of the image intensity along the vessel centerline and well outside a capillary, the signal-to-noise ratio (SNR) in the measurement data was approximately 5.5. All experiments reported here were recorded with an earlier and less optimized trajectory than described by equation (1) (which becomes apparent when Figure 1a and Figure 3b are compared).

The synthetic scan data was generated based on the numerical results from a two-phase model of the perfusion in a capillary network [6]. Artificial images similar to the experimental data were constructed from the instantaneous calculated positions of RBCs in the network (Figure 3b). In the simulation, the RBCs have a circular shape with a constant radius; the capillaries have a diameter of 5 μm and bifurcate at 120 degrees. The scanning trajectory is implemented according to equation (1) with the correct physical time and length scales. In the measurement data the RBCs appear not completely black, and a fluorescent signal from the capillary walls is visible (Figure 4). To emulate this, the synthetic RBC images were not set to black but to half the signal amplitude. In addition, the data was blurred with a low-pass filter and degraded with different levels of additive Gaussian noise to study the effect of varying signal-to-noise ratios (Figure 3c).

3 Results

The diversity of conditions in capillaries and the resulting differences in experimental data and image quality are illustrated in Figure 4. As a consequence, the parameters for post-processing have to be adapted and the minimum PIV-window size has to be found ad hoc for each set of data.

The error of the method is clearly a function of how accurately pairs of RBC sequences can be identified and located in the stack, i.e. of the accuracy of the PIV algorithm. Compared to traditional PIV, the synthetic RBCs are rather large (5-10 pixels) but only few reside in one search window. For these conditions, a rough estimate of 0.2 pixel can be given for the error in the determined shift [8]. This value changes significantly with image quality. As the images represent a stack of scans,

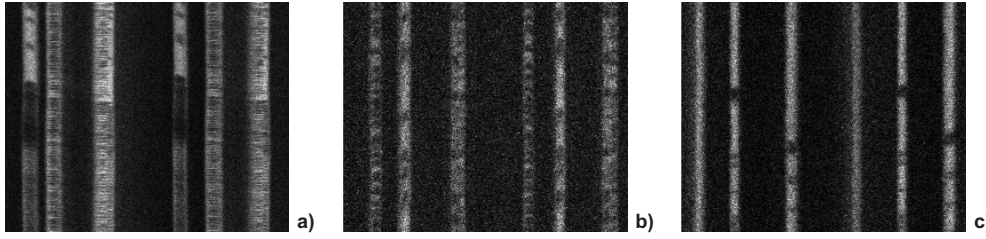


Fig. 4 In vivo two-photon microscopy raw data from a cerebral capillary network in mice (200 trajectory cycles shown only) for three different bifurcations and conditions. Using the capillary numbering of Figure 1a: (a) Relatively thick but few black sections could indicate low RBC velocities and numbers in vessel 1 but the significant vertical displacement observed between the two passes (1 and 4) indicate high velocities with clustering of RBCs. Numerous small black lines in vessel 2 show high RBC velocities and numbers. Panel (b) shows a more steady situation in all three vessels with relatively low velocities. (c) Shows a case with very few RBCs.

the time-increment between two pixels in the vertical direction is much larger than in horizontal direction. Errors in the lateral capillary position are therefore much less significant than the uncertainty in the vertical shift of RBC patterns.

With the PIV-error estimate and from the trajectory and time matrices, the uncertainty in the determined time interval Δt and distance Δx between the two crossings can be calculated as 0.2 ms and $0.4 \mu\text{m}$, respectively. Gaussian error propagation then yields the lower limit for the uncertainty in measured RBC velocity with $4 \cdot 10^{-6}$ m/s wherein the uncertainty in position clearly dominates. This estimate represents a lower limit for the accuracy as it neglects other error sources, e.g. measurement noise in the trajectory signal.

Figure 5 shows the measured in vivo blood flow velocity in each vessel of a converging and a diverging bifurcation as a function of time. In Figure 5a, the crosstalk between one feeding vessel and the draining vessel is clearly visible. In Figure 5b, single bifurcation events detected in the green channel are indicated with circles. As in the converging case, it can be observed that the velocity varies in the opposite sense in the daughter vessels while the in-flow velocity in the feeding vessel remains relatively constant.

The time-resolved RBC velocities for the three capillaries of a bifurcation in a simulated network are illustrated in Figure 6a. With the exact values known from the simulation, the temporal and spatial resolution as well as the accuracy of the method as a function of different parameters can be studied. A step-change in velocity was imposed at a $t = 1$ s in the simulation and the respective exact values are indicated on the ordinate. The data was processed with three separate lengths of PIV search windows. As expected, the graphs show for smaller search windows: (a) an increase in measurement noise, (b) the emergence of outliers due to a smaller number of RBCs (or none at all) in one window and (c) a higher resolution in time. At a scanning rate of 1300

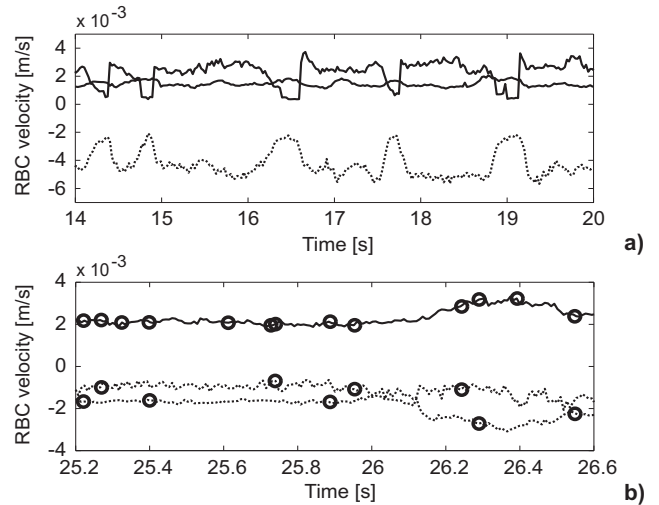


Fig. 5 RBC velocities measured from in vivo data of the cerebral capillary network of mice. (a) Shows a convergent bifurcation with two feeding vessels (solid lines), (b) a bifurcation with one feeding vessel (solid line) and two daughter vessels (dotted line). Single RBCs as detected in the green channel are highlighted with circles. RBCs that pass from the feeding vessel to a daughter vessel indicate single bifurcation events, vanishing RBCs indicate dropouts during post-processing.

Hz and conservatively assuming that the velocity is averaged over the entire length of a single PIV window, the time resolution is 25 ms for the smallest and about 100 ms for the largest window shown. While in Figure 6 the averaged velocities are in excellent agreement with the exact values for two capillaries, the value in the vessel with medium velocity is overestimated. The difference is about one order of magnitude larger than the above estimate for the PIV error. This type of error can be observed in some cases with synthetic data that is based on trajectories with a significant difference in path velocity between inner and outer circle. The unequal scanning speed results in a different number of sampling points across a capillary which increases the lateral uncertainty of the image correlation. An image

correction using the track velocity available from the trajectory data or applying an iterative window deformation scheme seems to eliminate this [9].

The decrease in uncertainty with increasing window size is shown in more detail for the three capillaries in Figure 6b. For all capillaries, the standard deviation reaches values of $5 \cdot 10^{-6}$ m/s for the largest window size, which is very close to the PIV error estimate. Interestingly, the error is smallest for the capillary with the lowest velocities (the leftmost in Figure 3b) which has the fewest RBCs in one search window. A possible explanation would be that for faster velocities and constant scanning rate, the tip of an RBC is less accurately captured.

The uncertainty of the method increases significantly for signal-to-noise ratios of the synthetic intensity images below 6 (Figure 6c). In the experiment, SNRs of 5.5 were observed which appears to be just acceptable. Noise added to the synthetic trajectory data is largely smoothed out in the interpolation step and has no significant impact on the error.

4 Discussion and Outlook

We have shown that driving scanning microscopes with double-circle trajectories allows simultaneous, time-resolved in vivo measurements of RBC velocity in all three branches of a capillary bifurcation. With some RBCs stained with a different fluorescent dye, single bifurcation events can be detected and related to the instantaneous quantities measured in the vessels. The achievable accuracy and time resolution of the method is close or equivalent to established methods like LS and RTLS but with the additional capability of measuring multiple capillaries simultaneously. Evaluating the ratio of dark and bright sections should yield the instantaneous hematocrit for each vessel.

With significant variation in scanning parameters, flow velocity and image quality, the post-processing parameters (e.g. PIV window size and search range) need adaptation and are currently adjusted manually and interactively until a (subjective) optimum is found. As a rule of thumb, a search window should include at least one entire RBC. This renders the time resolution of the method to some degree dependent on the measured velocity but also on the hematocrit. Implementing a procedure to calculate the local hematocrit (e.g. by relating the spatial frequency of the dark and bright sections to the velocity) will presumably allow to automate the post-processing further. Further work is also needed to improve the reliability and the degree of automatization with which bifurcation events are identified in the algorithm.

The artificially generated images are of great value to assess the performance of the method. Trajectory, scanning parameters, RBC flux and velocity can be adjusted without the constraints of an experimental setup. With the trajectory optimized for maximum distance between the capillary crossings, the difference in track speed on the inner and outer circle of the trajectory becomes significant and results in a different number of sampling points across a capillary. This can be the cause of errors as it can shift the cross-correlation peak and reduces its magnitude. Possible solutions are a correction of the images prior to post-processing using the trajectory data, the use of an iterative window deformation scheme or a slow down of the scanning speed along the outer circle.

The capability to measure in vivo RBC velocity, flux and local hematocrit simultaneously in individual vessels of a capillary bifurcation can become a valuable tool in neurobiological research. In particular, the method allows relating the velocity in the vessels to the ratio of hematocrit separation as discussed, e.g. by Pries et al. [10].

References

1. Denk W, Strickler JH and Webb WW, Two-photon laser scanning fluorescence microscopy, *Science*, 248, 73-76 (1990)
2. Helmchen F and Denk W, Deep tissue two-photon microscopy, *Nat Methods*, 2, 932-940 (2005)
3. Kamoun WS, Chae SS, Lacorre DA, Tyrell JA, Mitre M, Gillissen MA, Fukumura D, Jain RK and Munn LL, Simultaneous measurement of RBC velocity, flux, hematocrit and shear rate in tumor vascular networks, *Nat Methods*, 7, 655-660 (2010)
4. Kleinfeld D, Mitra PP, Helmchen F and Denk W, Fluctuations and stimulus-induced changes in blood flow observed in individual capillaries in layers 2 through 4 of rat neocortex, *PNAS*, 95(26), 15741-6 (1998)
5. Hart DP, Super-Resolution PIV by Recursive Local-Correlation, *Journal of Visualization*, 10 (1999)
6. Obrist D, Weber B, Buck A and Jenny P, Red blood cell distribution in simplified capillary networks, *Phil. Trans. R. Soc. A*, 368, 2897-2918 (2010)
7. Peppiatt CM, Howarth C, Mobbs P and Attwell D, Bidirectional control of CNS capillary diameter by pericytes, *Nature*, 443(7112):700-4 (2006)
8. Raffel R, Willert CE, Wereley ST and Kompenhans J, *Particle Image Velocimetry* (2nd ed.), 166-169, Springer, Berlin (2007)
9. Scarano F, Iterative image deformation methods in PIV, *Meas. Sci. Technol.* 13, R1R19 (2002)
10. Pries AR, Ley K, Claassen M and Gaehtgens P, Red cell distribution at microvascular bifurcations, *Microvasc Res*, 38, 81-101 (1989)

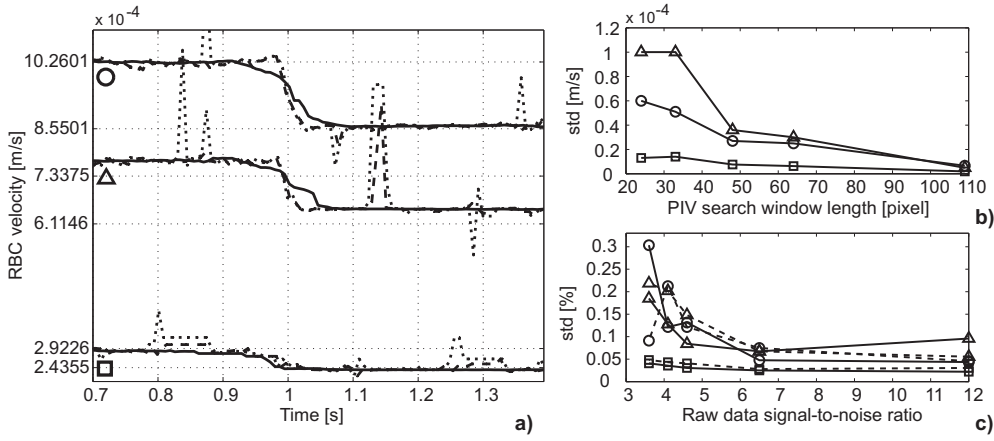


Fig. 6 The calculated RBC velocity magnitudes for the three capillaries of a bifurcation from synthetic data including a sudden change in velocity at 1 s a). The solid line represents a PIV-search window length of 109, the dashed line 48 and the dotted line 33 pixels, respectively (the exact values extracted from the simulation are shown on the ordinate). b) Illustrates the decrease in measurement noise with increasing search window length. Both figures are without noise added to the data. c) The decrease of the uncertainty with increasing signal-to-noise ratio. The dashed line shows the effect of noise added to the trajectory data to match the experimental conditions.